



## ORIGINAL PAPER

**IDENTIFYING FAULT SYSTEM AND BASEMENT DEPTH USING AEROMAGNETIC DATA BENEATH THE JAHAMAH PLATFORM, NE SIRT BASIN, LIBYA****Sufian KAHOU<sup>1</sup>\*, Akhmal SIDEK<sup>1</sup>, Abdelhakim ESHANIBLI<sup>2,4</sup>, Fouzie TREPIL<sup>3,4</sup>, Mohd Zaidi Bin JAAFAR<sup>1</sup>, Moamen HASSAN<sup>1</sup>, Hussin GHANUSH<sup>2</sup> and Lutfi DUGDUG<sup>5</sup>**<sup>1</sup> Petroleum Dep., School of Chemical and Energy Engineering, University of Technology Malaysia, 81310, Johor, Malaysia<sup>2</sup> Libyan Petroleum Institute, Tripoli, 6431, Libya<sup>3</sup> Geophysics Dept., Faculty of Science, University of Tripoli, PO Box 13275, Tripoli, Libya<sup>4</sup> School of Physics, University Science Malaysia, 11800, Pulau Penang, Malaysia.<sup>5</sup> Waha Oil Company, Tripoli, Libya.\*Corresponding author's e-mail: [Sufiankahoul2@gmail.com](mailto:Sufiankahoul2@gmail.com)**ARTICLE INFO****Article history:**

Received 20 January 2022

Accepted 30 March 2022

Available online 21 April 2022

**Keywords:**Magnetic  
Euler Deconvolution  
Sirt  
Jahamah  
Libya**ABSTRACT**

The Jahamah Platform is a part of a structural depression called the Sirt basin, located in the northern central part of Libya. The Jahamah Platform spans latitude 29.95° N to 30.55° N and longitudes 19.32° E to 19.77° E with an estimated area of about 2,187 km<sup>2</sup>. Libyan Petroleum Institute provided the data of aeromagnetic that was used in this study. The data was used to study the structure beneath the Jahamah Platform by using Oasis montaj software. Various filters from the software have been applied to enhance determining the fault system within the study area. An RTP filter was applied to the magnetic data to construct a reduction to the pole anomaly map. The subsurface structural elements underneath the study area were identified using Total horizontal derivative (THD), CET analysis, and Euler deconvolution. 2-D forward modelling of the area was constructed based on gravity data, and then the basement depth was estimated to range from 2.2 km to 3.1 km based on the model. Based on the interpretation of the constructed maps, the area has a number of faults that trend in NE-SW, NNW-SSE, N-S and NW-SE and faults depth ranging between 790 m to 3102 m.

**1. INTRODUCTION**

The magnetic method, which is more colloquially known as a geomagnetic method, tests changes in the magnetic susceptibility (the degree of magnetisation in the magnetic field) of the rocks. It is a non-destructive and passive method (Hinze et al., 2013). The acquired magnetic field is superimposed on the Earth's magnetic field, producing a minor distortion or anomaly. Variations in the amplitude and orientation of the ground determine the magnitude and shape of the local anomaly caused by the mass of rock (Hinze et al., 2013). Various studies have been conducted within or around the area (Saheel et al., 2010a,b, 2011; Baask et al., 2009; Ghanush et al., 2014; Saleem, 2015; Wang et al., 2016; Ghanush, 2019; Eshanibli et al., 2020; Eshanibli et al., 2021). The Al Jahamah Platform shapes a prominent ridge separated from the Zelten Platform by the Al Wadayat Trough. There are no sufficient studies about the Jahamah Platform as a single area. Also, the complex geological settings of the Jahamah Platform makes it too difficult to understand the structural trends within and around the platform. These structures are thought to play an important part in the geometry and properties of the hydrocarbon basin (Eshanibli et al.,

2021). Unfortunately, the degree of understanding of structural evolution is insufficient until now. As a result, attempts must be made to define the area's structural pattern using all existing data. The Jahamah Platform, which covers an area extending from longitudes 19.32° E – 19.77° E and latitudes 29.95° N – 30.55° N with an estimated area of around 2186 square km. The Jahamah Platform is part of the Sirt Basin, a structural depression located in the north-central part of Libya with an area of 230,000km<sup>2</sup> (Hallett, 2002). The Mediterranean Sea bounds the Jahamah Platform from the northwest with a cost of 300 km long, Ajdabiya Trough from the east, and Zelten Platform from the west (Fig. 1). Sirt Basin is the youngest sedimentary basin and is predicted to be one of the most promising areas in terms of hydrocarbon in Libya (Hallett and Clark-Lowes, 2017). The Jahamah platform is part of the Sirt Basin, and most of the studies and researches are done on the Sirt Basin as a whole and do not focusspecifically on the Jahamah Platform as a single part. So, conducting such a study about the area will be helpful for future studies and researches related to geology, geophysics and oil and gas exploration.

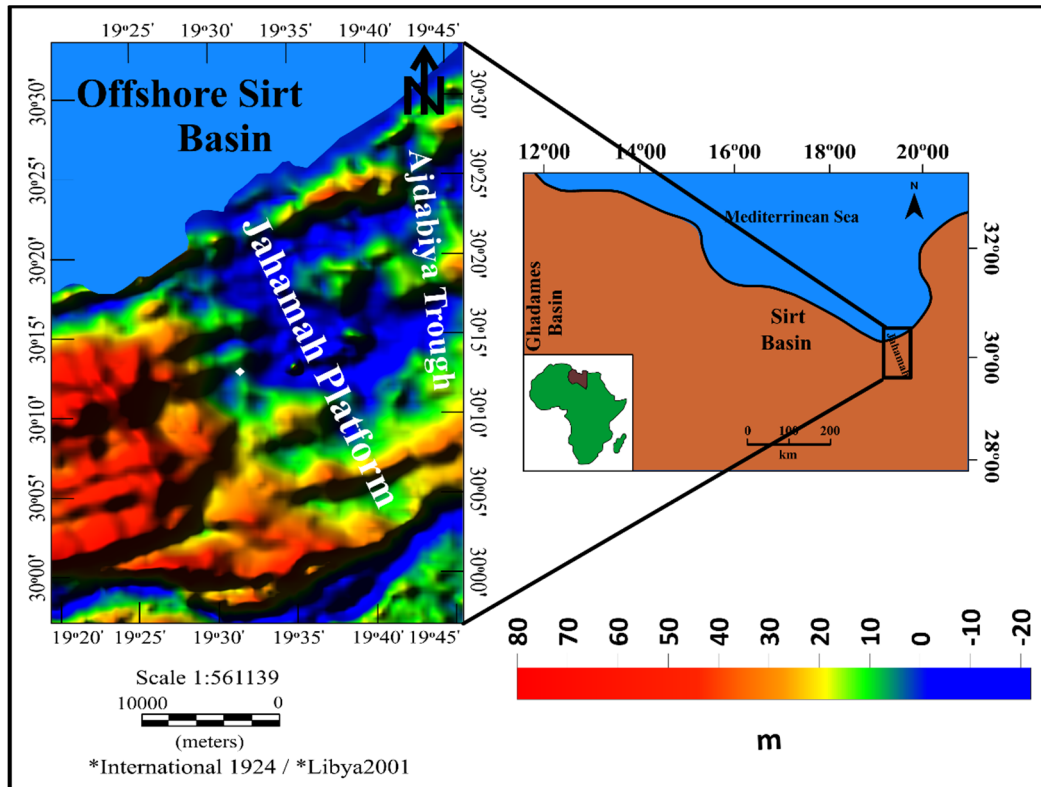


Fig. 1 Elevation and location map of the Jahamah Platform.

## 2. GEOLOGICAL SETTING

The complicated geological structure of the Sirt Basin (Fig. 2) is a result of the collapse of the Sirt Arch (Finetti, 1985; Hallett and El Ghoul, 1996) and is composed mainly of NW-SE trending Cretaceous to Eocene rift structure overlain by a thick sequence of Cenozoic post-rift strata (Baird et al., 1996). Authors like Conant and Goudarzi (1967), Klitzsch (1971) and Massa et al. (1977) have studied the geology of the Sirt Basin. During the Early Palaeozoic, the Sirt Basin was an arch (Shaaban and Ghoneimi, 2001). After Pan-African orogeny, quartzitic sediments were deposited in the Kalanshiyu Trough (Hallett and Clark-Lowes, 2017). During the Hercynian Orogeny with alkaline magmatism (Permian-Jurassic) caused thinning of the Silurian sequence across the Sirt area to form the Hercynian uplifts, which trend North-East from Chad to Cyrenaica (Vail, 1991).

The collapsing of Sirt Basin occurred in the Early cretaceous by several tectonic movements, such as the Caledonian orogeny and the westward movement of the African plate relative to the European plate (Ghanush et al., 2014). This created an extension zone at the crust and caused active subsidence resulting in the Sirt Arch (Burke and Dewey, 1973; Saleem, 2015). The Sirt Basin is a form of continental rifting (Extensional) region and is part of the Tethyan rift system (Ahlbrandt, 2001). During the Cretaceous period, the Sirt Basin region witnessed stretching and down faulting. Subsidence and block faulting on a large scale began in the Late Jurassic/Early Cretaceous

(Abadi, 2002). The basin was reactivated both in the Late Cretaceous to early Palaeocene and in the Oligocene to Miocene (Gumati and Kanen, 1985; van Der Meer and Cloetingh, 1993). Some authors such as Burke and Dewey (1973) proposed that in Sirt Basin occurred during the early Cretaceous, in weak zones among two African sub-plates as a result of the extensional movement that resulted in the collapse of the pre-existing Sirt Arch. The Northwest-Southeast faulting system with horst and graben patterns occurred during the Early Cretaceous and reached a climax throughout the Tertiary period (Duronio and Colombi, 1983). The Sirt Basin's NW-SE structural characteristics evolved during the Late Cretaceous and it was associated with crustal extension in the NE-SW direction, which illustrates the length of the West African rift system running from Libya's Sirt Basin to Niger's Benue Trough (Abadi, 2002; Abadi et al., 2008). The Hercynian Orogeny occurred at the Late Carboniferous to Early Permian (400 - 280 Ma), creating a wide arching area within the Sirt Basin (Hallett and El Ghoul, 1996). The NW-SE orientation of the structural features at the Sirt Basin was developed by the crustal extension, which occurred in the early upper Triassic to the Early Cretaceous. The changes in the movement of the African Plate associated with the change in the movement of the Eurasian resulted in a compressional event during the Santonian period between 98 - 83.5 Ma (Anketell, 1996; Abadi, 2002; Abadi et al., 2008). The Jahamah Platform is separated from the Nuwfalayah High by

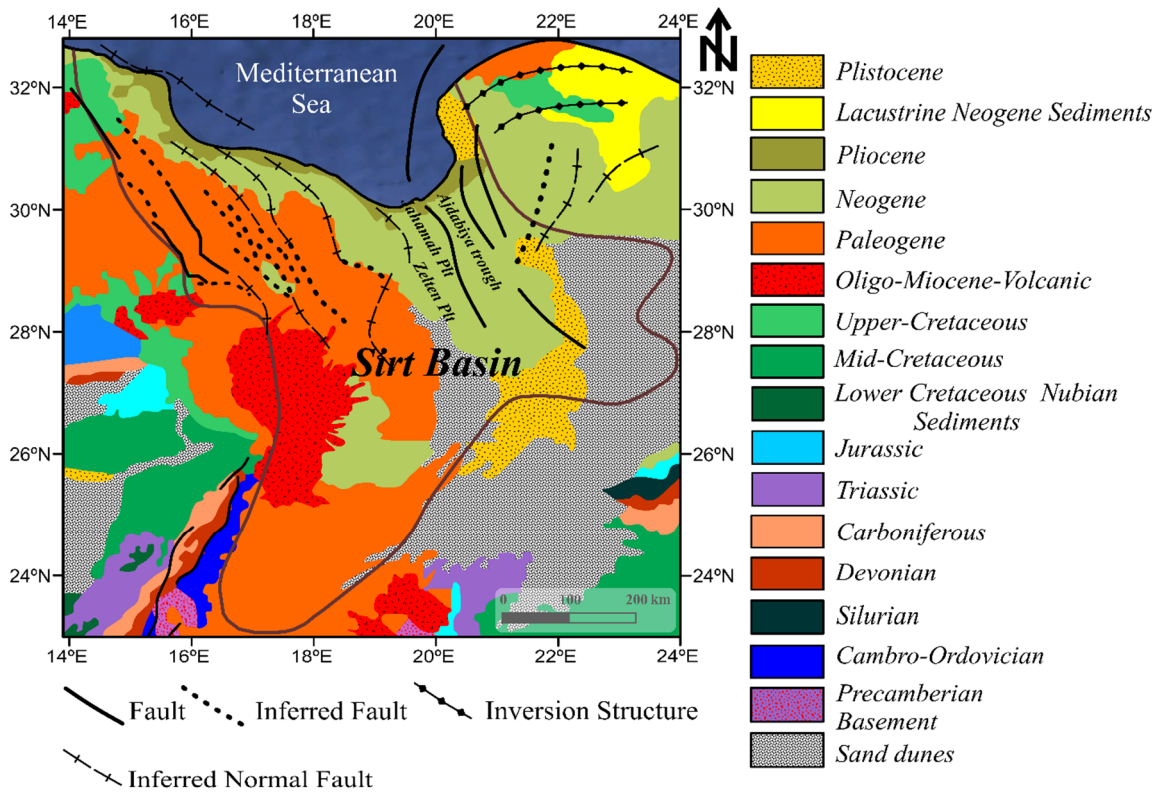


**Fig. 2** Sirt Basin's geological map showing the Jahamah Platform in the north.

major faults trending NW-SE, extending about 600 m at the southern boundary with Maradah Trough (Hallett and Clark-Lowes, 2017). Another saddle north of the Attahadi gas field separates the Jahamah Platform from the Zelten Platform, located between the two platforms (Gumati and Kanen, 1985). On the Jahamah Platform, there seems to be a significant unconformity between the Cretaceous and Palaeocene. It looks that the Danian strata is absent and that the whole Palaeocene thins fast as it moves north (Hallett, 2002). During the Eocene, the platform was raised, the faults were reactivated, and the platform was exposed to regional tilting due to Alpine tectonic activity (Hallett and El Ghoul, 1996).

### 3. MATERIALS AND METHOD

#### 3.1. DATA

The data used in this study was provided by the Libyan Petroleum Institute (LPI). LPI is an institution under the National Oil Corporation (NOC). It was established in 1977 and known as Petroleum Research Centre (PRC) located in Tripoli, Libya. The LPI originally obtained the data from the African Magnetic Mapping Project (AMMP). For the continent of Africa, the AMMP collects all available aeroplane, ground, and marine magnetic data (Eshanibli et al., 2020). Both the flight lines and the data points on each line are separated by 1.0 km. In the N-S direction, there were 89 flight lines with approximately 95 data points each, which makes the total 8,486 magnetic data points.

#### 3.2. MAGNETIC DATA PROCESSING AND MODELLING

Magnetic datasets will be imported into Oasis montaj in "XYZ" spreadsheet format. Following the import of the data into oasis montaj, the data will be gridded whereby Gridding interpolates the data file's position (x, y) and (z) columns to construct a normal and smoothly sampled representation of the positions and data. The Kriging method is used to grid magnetic data as the data was taken as a line and perpendicular to the structure orientation within the area. The gridding cell size used in this study was 100.

The total magnetic intensity (TMI) was obtained by gridding the magnetic data by the Kriging method (Fig. 4a). RTP map is then constructed by applying reduced to the pole filter on the TMI to make the magnetic anomalies exactly above their source bodies and without any distortion. In most cases, the RTP transformation assumes that the total magnetisation of most rocks aligns parallel or anti-parallel to the Earth's primary field (Keller, 1986; Blakely, 1996).

Further processing on the datasets was done by applying filters and analysis such as the reduction to the pole filter, Centre for Exploration Targeting grid analysis (CET), Total Horizontal Derivative and High Pass filter. Lastly, using Oasis montaj (GM-SYS), the 2-D modelling of the area was constructed based on the magnetic data. Figure 3 shows the methodology of this study.

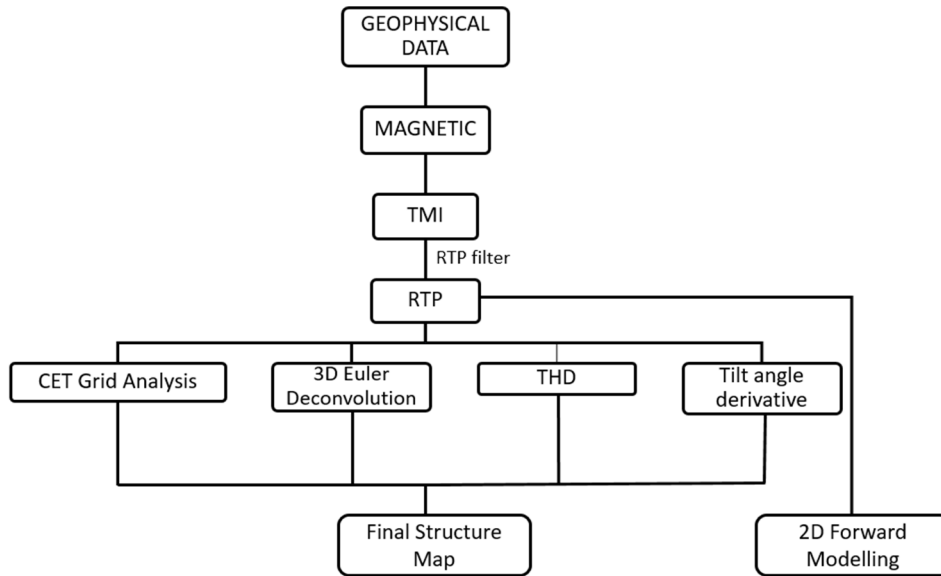


Fig. 3 Methodology flow chart.

- Total Horizontal Derivative (THD) of Magnetic Anomaly

According to Eshanibli et al. (2020) the Total Horizontal Derivative (THD) (Eq. 1) is a popular method for analysing magnetic and gravity data. When applying to gravity data, the THD aids in the location of density boundaries and the definition of geological contacts. The THD technique, on the other hand, is used to delineate susceptibility boundaries using magnetic data. Since it only needs the measurement of the field's two first-order horizontal derivatives, the THD has a low susceptibility to noise in the data. As opposed to the vertical gradient method, which is only useful for shallower structures, the method is also excellent at delineating either shallow or deep sources (Saadi et al., 2008).

$$THD(x, y) = \sqrt{\left(\frac{\partial g}{\partial x}\right)^2 + \left(\frac{\partial g}{\partial y}\right)^2} \quad (1)$$

Whereby  $THD(x, y)$  represents the magnitude of the horizontal derivative, while  $g$  is the gravity or magnetic anomaly,  $\frac{\partial g}{\partial x}$  and  $\frac{\partial g}{\partial y}$  are the partial derivatives of  $g$  with respect to  $x$  and  $y$ .

- CET Grid Analysis

A CET grid analysis expansion is an algorithm tool to improve, locate and carve discontinuities with potential field data. It has been developed by the Exploration Centre group (CET) at Curtin University. It enables fast and impartial pattern detection in the most important data sets. The density discontinuity can be identified using a combination of texture analysis and bilateral symmetric function detection by Holden et al. (2012). This study will use the CET analysis for the magnetic data. The wavelength of the

smallest filter will be set to 3 cells, the number of filter scales to 3. The congruency strength value will be fixed at 5 and the focus for all angles was determined.

$$E = -\sum_{i=1}^n P_i \text{Log } \rho_i \quad (2)$$

After normalising the histogram of  $n$  bins, the probability  $\rho$  is obtained.

- Tilt Angle Derivative

The tilt angle derivative is implemented to distinguish magnetic and gravity anomaly on the basis of a set of vertical and horizontal derivatives of the magnetic and gravity (Ming et al., 2021). When the density contrast of causative mass is positive the tilt angle over the source will be positive and further than the source bounds will be negative. The tilting angle value of the horizontal derivatives is around zero near the edge with a vertical derivative value of zero. Cooper and Cowan (2006) claim that the interpretation of tilt angle is easier than the analytical signal phase angle due to the fact that it ranges from -90 to +90 to total (Miller and Singh, 1994; Eshanibli et al., 2020).

- Euler Deconvolution

Euler deconvolution is an automated technique used for magnetic and gravity data analysis. In this analysis the structural index (SI) for gravity will be set to 0 and the magnetic data set to 1 Euler deconvolution. The SI is an exponential factor which describes the nature of the causative source and for various geological bodies is different (Table 1). The overall tolerance of the percentage depth determining the solution accepted is 15%. The window area in grid cells was determined by an 8\*8 grid cell, which was sufficiently wide to contain many anomalies. For gravitational anomalies, the highest altitude was sea level and magnetic anomaly was 1 km above terrain.

**Table 1** Structural index (SI) for magnetic (Reid et al., 2004).

Source	Magnetic
Fault	1
Contact	0
Sphere	3
Horizontal	2

• 2-D Modelling

The GM-SYS modelling extension of the Oasis montaj will be used to produce the geological models in the Jahamah Platform. The GM-SYS enables a model to be generated and a gravity and magnetic validation testing to be performed for the measurements observed. The GM-SYS helps in determining depth to basement by determining rock densities and magnet susceptibility. The magnetic susceptibility values are obtained from (Talwani et al., 1959; Blakely, 1996; Ghanush, 2019; Eshanibli et al., 2020) and are adjusted until the best fit is achieved between the observed and calculated values.

**4. RESULTS AND DISCUSSION**

The TMI map (Fig. 4a) shows a high magnetic anomaly within the central part of the study area and extends to the northeast ranging from 34.0 nT to 40.6 nT, which depicted the large scale of fault system within the Platform. While it shows that the Ajdabiya Trough has a low magnetic anomaly ranging from 12.0 nT to -13.8 nT in the south-eastern part of the

Jahamah. This low magnetic anomaly was extended from surrounding areas such as the central part of the Ajdabiya Trough, which was affected by the subsiding during the lower Cretaceous rifting (Ghanush, 2019).

Magnetic anomalous field zone can be isolated using the reduction to the pole (RTP) transformation, its common, to apply RTP transformation technique on the magnetic data to reduce polarity effects. The RTP map (Fig. 4b) shows the existence of high and low-frequency anomalies in the magnetic field of the region. The map shows high anomaly values in the central and northern parts of the study area, ranging from 30.0 nT to 65.4 nT. This high anomaly refers to the depth of the basement, which might indicate shallow basement depth. The southwestern part of the area is characterised by low anomaly magnetic values ranging from -31.5 nT to 16.7 nT. For modelling purposes, four profiles were taken across the Jahamah Platform. The black lines on the RTP map represent the profiles from which the 2D models have been constructed. The profiles for the modelling were taken on the RTP map due to the magnetic anomaly in TMI not exactly above the causative body, which would lead to misinterpretation after applying the modelling.

To the north-eastern part of the study area where the Ajdabiya Trough is located, the area is characterised by a low anomaly which may refer to a deep basement depth. The high anomaly values refer to a strong NW-SE trending fault which refer the

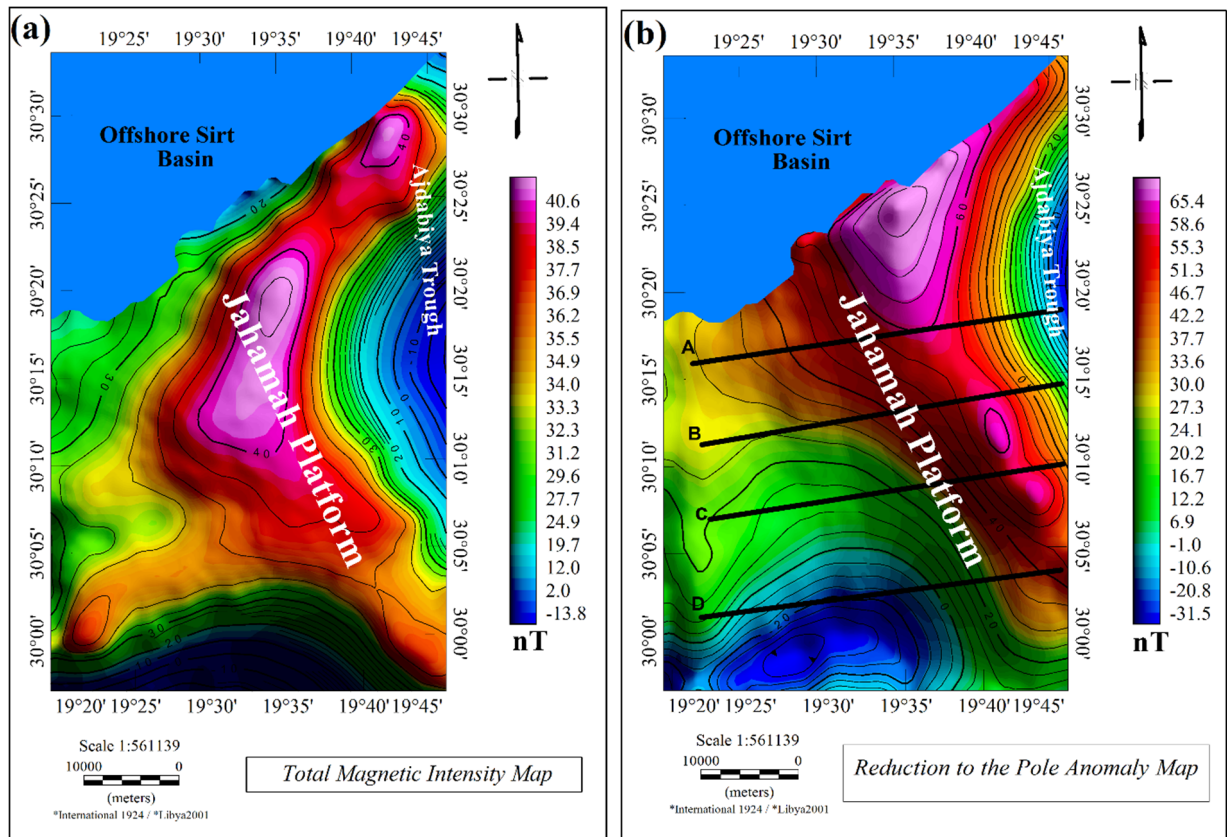


**Fig. 4** (a) TMI map (b) RTP anomaly map; the black lines (A to D) refers to the 2D profiles taken for the 2D modelling.

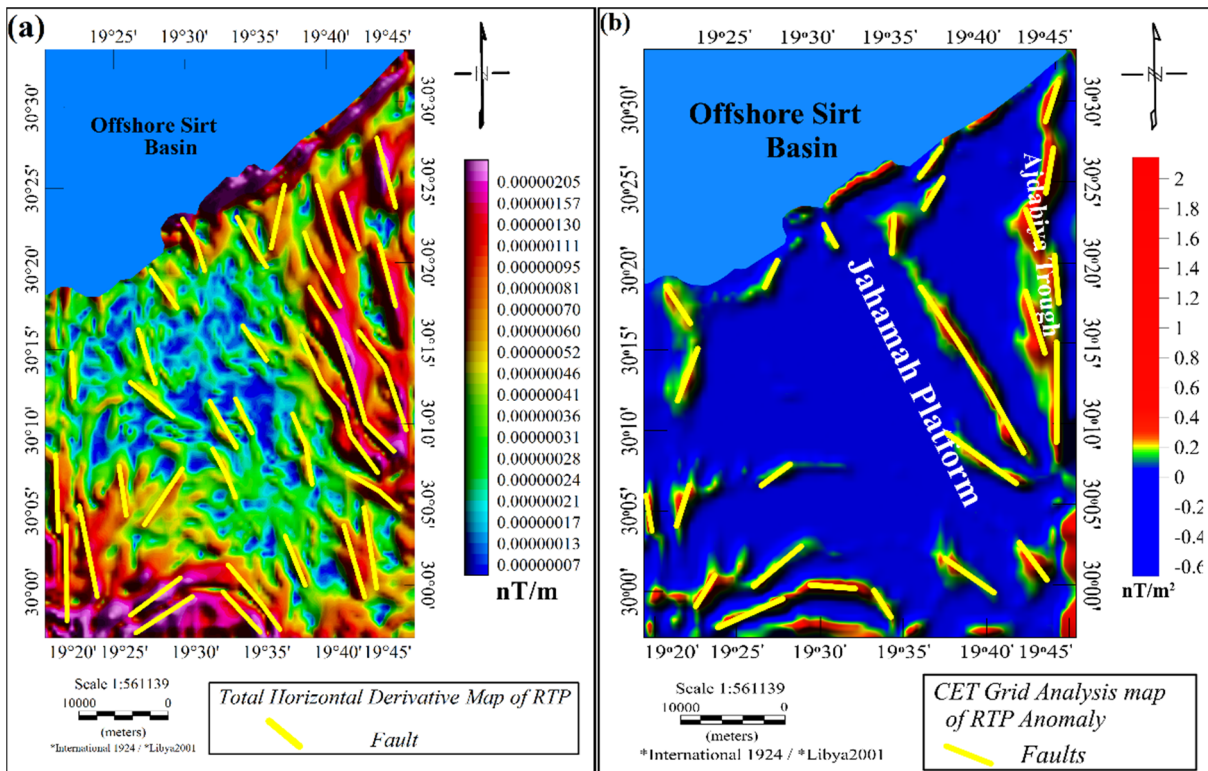


**Fig. 5** (a) Total horizontal derivative and (b) CET grid analysis.

major tectonic event that occurred to the African plate and Eurasian during the Santonian. In addition, this NW-SE trending fault resulted from the third phase of rifting that formed the Sirt Basin (Anketell, 1996; Abadi, 2002; Abadi et al., 2008).

The CET grid analysis and the Total horizontal derivative are applied to the RTP magnetic anomaly. The result of both techniques shows a variety of faults that trend NNW-SSE, NW-SE, NE-SW and N-S (Figs. 5a,b). These different trends refer to various tectonic movements, such as the extension movement that occurred within the Late Jurassic to the Upper Cretaceous and the movement of African plate and Eurasian during the Santonian. The northwest-southwest fault may have contributed to the basement development beneath the Jahamah Platform. Moreover, the Jahamah Platform's northern NE-SW tectonic expansion is more recent than the one within the Ajdabiya Trough, presumably due to the late stage of development of the Sirt Basin during the collision of the African and Eurasian plates (e.g. Ghanush, 2019).

Euler solution maps are created from the magnetic anomaly within Oasis Montaj and the window size of 8\*8 (64 cells). The structural index was set at different values (0, 1, 2, and 3) to investigate the best solution that can be obtained (Fig. 6). The solution with SI=2 and SI=3 give very scattered solutions which do not represent any subsurface structures such as faults. On the other hand, the solution of SI=0 gives the major faults overlaid on the edge of the anomaly of RTP. Therefore, the chosen

solution was with SI of 1 with a maximum depth tolerance of 15 % which shows the best structural trend. The map of Euler deconvolution solution of RTP grid (Fig. 7) illustrates that the depth ranges between 790 m to 3102 m. the solution map of Euler confirmed the trend faults observed from the CET and THD. This solution shows that some faults might have penetrated the basement rock within the study area and this structure pattern might be explained by a reactivated Hercynian or older basement structure. (e.g. Eshanibli et al., 2020 and 2021).

The tilt angle derivative approach aids in determining potential field anomalies of causal source edges (Dogru et al., 2017; Putri et al., 2019). The tilt angle has a positive value if the density/susceptibility of the causative body is positive and negative value outside of the causative body limits. The tilt angle (Fig. 8) of the study area shows the presence of geological contact believed to be a group of faults, with dominant trend orientations NW-SW, NE-SW and N-S. These findings corresponded with the findings of some previous studies (e.g. Ghanush, 2019; Ghanush et al., 2014) that reported the rift phases that occurred within sirt basin such as Pre-rift, Syn-rift and Post-rift.

The structure map (Fig. 9) of the Jahamah Platform indicates the different trend faults that have been interpreted from the THD, CET and Euler magnetic. The faults in the map trend mainly in, northwest-southeast, northeast-southwest, north northwest-south southeast, and north-south. These faults indicate various tectonic events, such as those

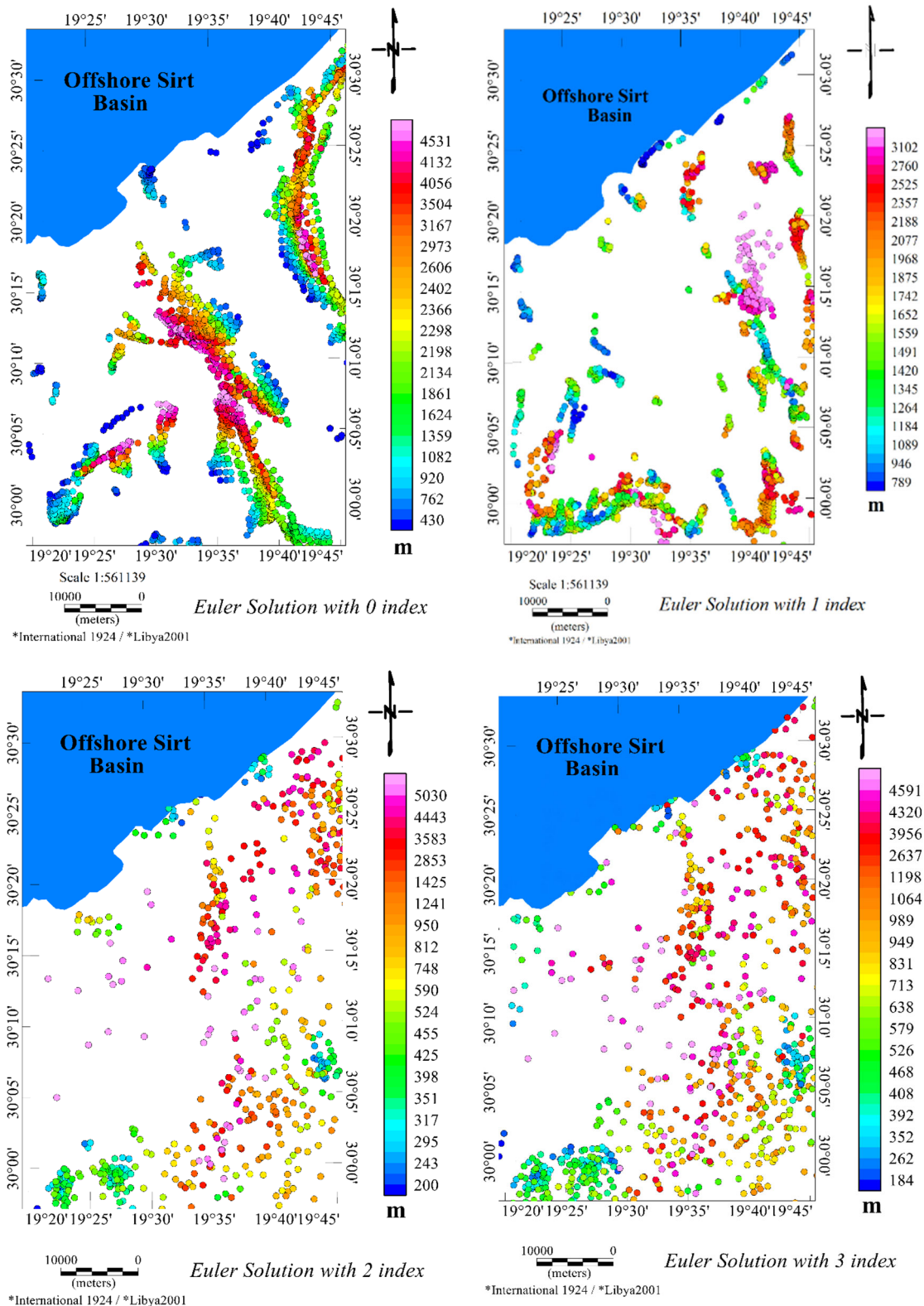


**Fig. 6** The different solutions of 3D Euler deconvolution coming from the different SI values of 0, 1, 2 and 3.

that occurred during the Early Cretaceous period and resulted in crustal expansion. And some of the faults might be the result of the first rifting episode, which occurred in the Early Palaeozoic.

The four profiles of the 2D-Forward modelling are taken along the Jahamah Platform as represented

on the RTP map (Fig. 4b) by black lines. Profile A (Fig. 10a) was taken with a length of 39.8 km west to east. The estimated basement depth of profile A ranges from 2.2-2.4 km. Moreover, the B profile (Fig. 10b) has a length of 39.8 km and basement depth of 2.2 - 2.8 km. Also, profile C (Fig. 10c) with profile lengths

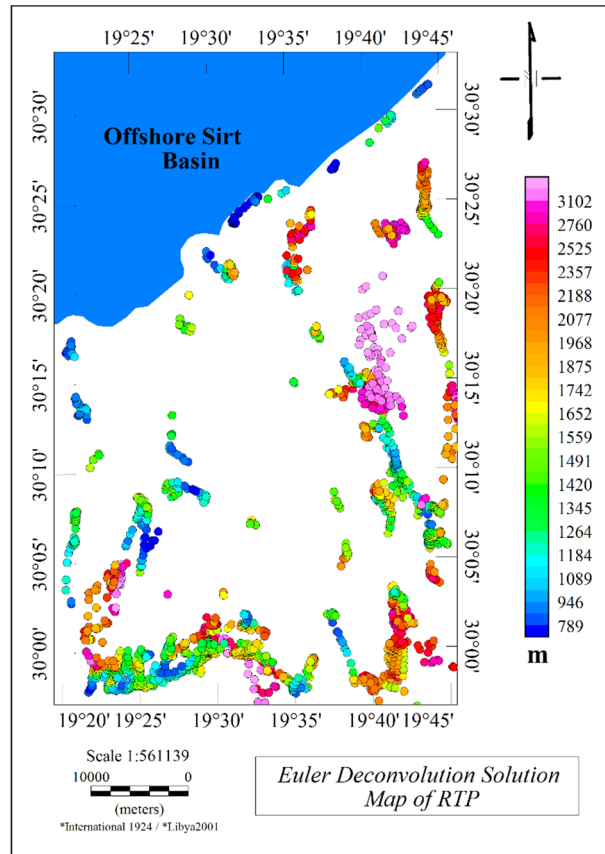


Fig. 7 The chosen 3D Euler deconvolution solution map of the magnetic anomaly of the Jahamah Platform (W=8, SI=1).

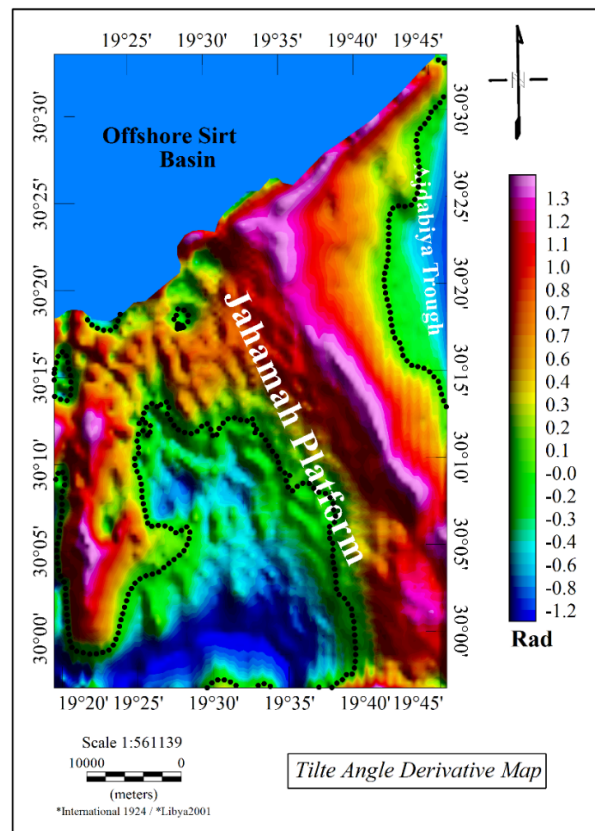
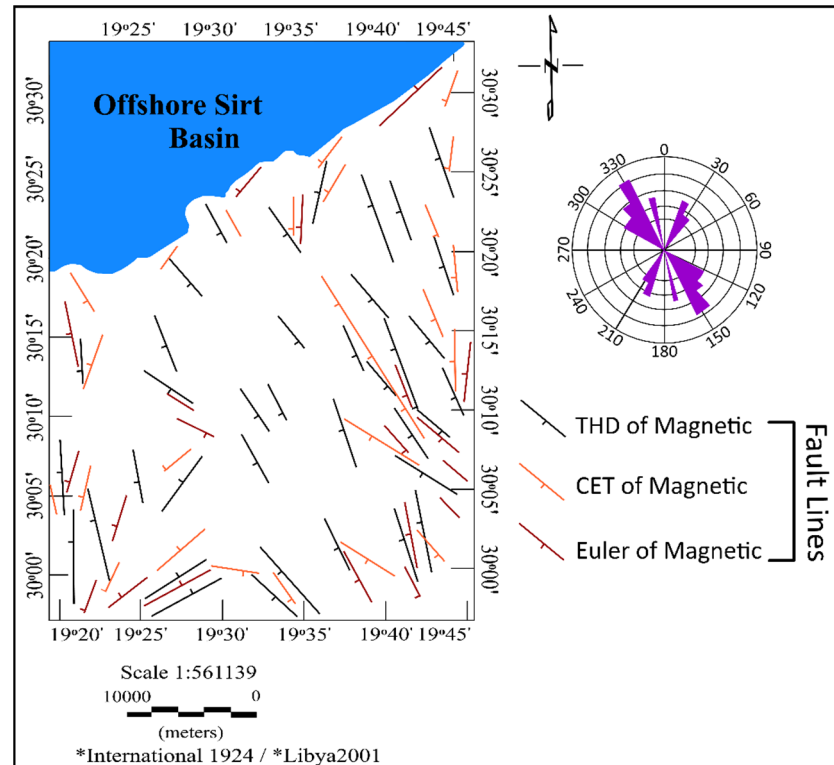


Fig. 8 Tilt angle derivative RTP map of the study region.





**Fig. 9** Structural map showing the faults from THD, CET and Euler deconvolution.

of 39.8 km shows an estimated depth of 2.2 - 2.9 km. Lastly, profile D (Fig. 10d) has a length of 37.7 km and indicates a deeper basement depth ranging from 2.3 km to 3.1 km.

By comparing with RTP map, profile A, B and C show the shallowest basement depth, which explains the high magnetic anomaly from RTP that indicates a shallow basement. On the other hand, profile D gives the deepest basement depth between the four profiles, which explains the low magnetic anomaly from the RTP, representing a deeper basement than the high magnetic anomaly region. The Zelten platform is the neighboring area of the Jahamah Platform from the northwest-southeast, and according to Hallett and Clark-Lowes (2017), it was estimated that the basement of the Zelten Platform is in the Upper Cretaceous. Therefore, since the Jahamah Platform is a continuation of the Zelten Platform on the geological map, it is expected that the basement of the Jahamah Platform is in the Upper Cretaceous layer. Finally, to validate the constructed models, the depth results were compared to the top Cretaceous map (basement for Zelten and Jahamah) from Hallett and Clark-Lowes (2017), and the results are almost similar. According to Hallett and Clark-Lowes (2017), the range of basement depth ranges from 2.4-3 km, while the constructed profiles show a range of 2.2-3.1 km. The values of susceptibility of basement and sediments values used in these profiles were estimated from some previous studies that have been done on the surrounding areas of the Jahamah Platform, such as (Ghanush, 2019; Eshanibli et al., 2020).

## 5. CONCLUSION

Various maps have been created as a result of using various enhancing techniques. The distribution of different anomalies can be seen in the RTP map. Different features with variable magnetic susceptibilities are the cause of these various anomalies. The THD and CET grid analysis of reduction to the pole magnetic anomaly show a group of faults trending in the NW-SE, NE-SW, N-S, and NNW-SSE. The fault trending NW-SE could have aided in forming the basement beneath the Jahamah Platform. Euler deconvolution of gravity and magnetic anomaly show different trending faults with different depths ranging from 790 m to 3102 m. The Tilt angle map shows a similar trend as those obtained from THD and CET grid analysis of the RTP map. According to the 2D modelling profiles the basement depth of the Jahamah Platform ranges between 2.2 km to 3.1 km. All these findings of faults represent the rift system that formed the reservoirs within the Sirt Basin during the Cretaceous period (Ghanush et al., 2014). So, identifying these faults is useful for those who are interested in the geology as well as in oil and gas exploration of the area in the future.

## ACKNOWLEDGEMENTS

We would like to express our gratitude to those who made the data available to be used like the LPI and NOC. Additionally, we would like to express our appreciation for the efforts of our reviewers, who have contributed to the improvement of the overall quality of this paper.

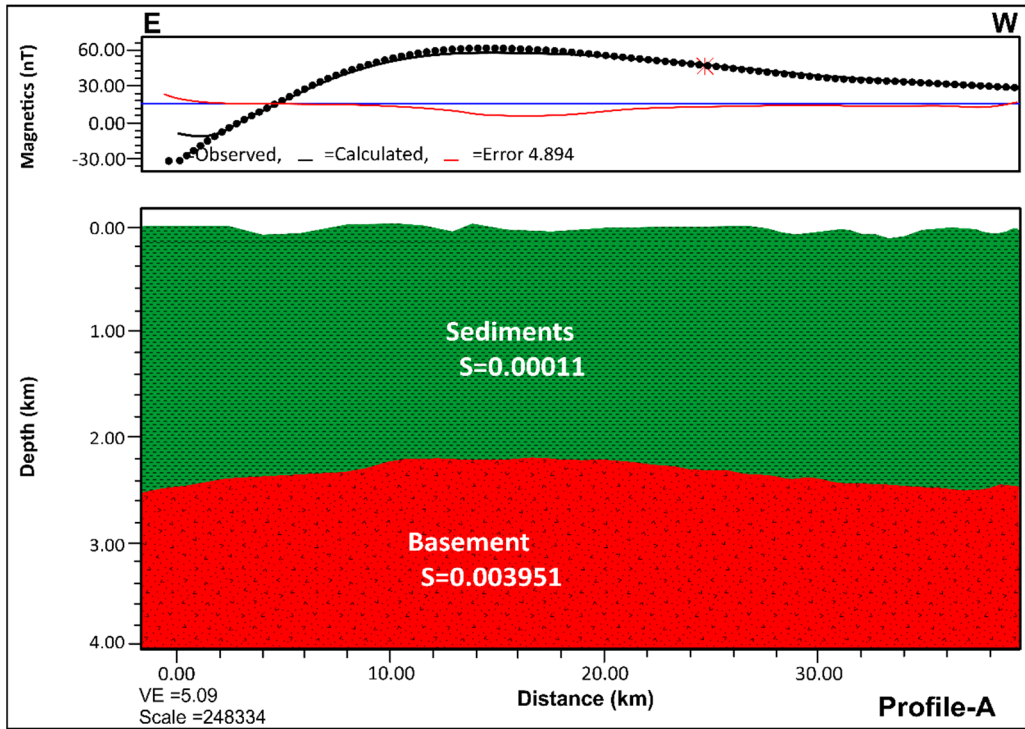


Fig. 10a 2D-Forward modelling profile A.

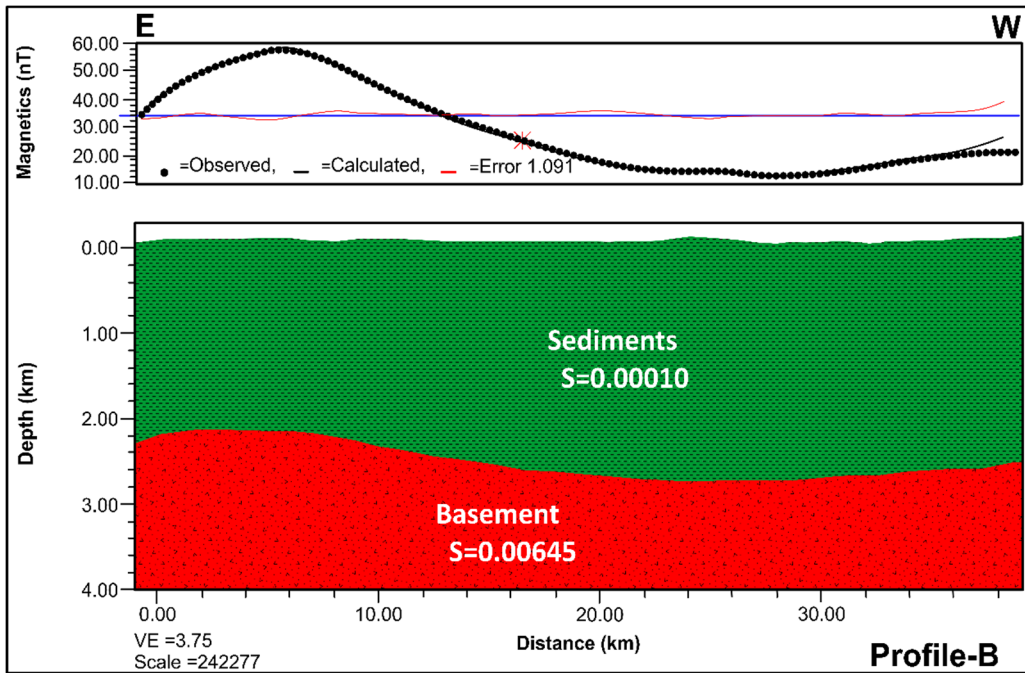


Fig. 10b 2D-Forward modelling profile B.

REFERENCES

Abadi, A.M.: 2002, Tectonics of the Sirt Basin. Inferences from tectonic subsidence analysis, stress inversion and gravity modelling. Ph.D Thesis, Vrije University Amsterdam, Netherlands.

Abadi, A.M., van Wees, J.-D., van Dijk, P.M. and Cloetingh, S.A.: 2008, Tectonics and subsidence evolution of the Sirt Basin, Libya. *AAPG Bull.*, 92, 8, 993–1027. DOI: 10.1306/03310806070

Ahlbrandt, T.: 2001, The Sirte Basin province of Libya: Sirte-Zelten total petroleum system. *Bull. U.S. Geol. Surv.* Retrieved from <https://pubs.usgs.gov/bul/b2202-f/b2202-f.pdf>

Anketell, J.M.: 1996, Structural history of the Sirt basin and its relationship to the Sabrata basin and Cyrenaica platform, northern Libya. In: Salem, M.J. et al. (eds.), *The Geology of the Sirt basin, III*, Elsevier, Amsterdam, 57–89.

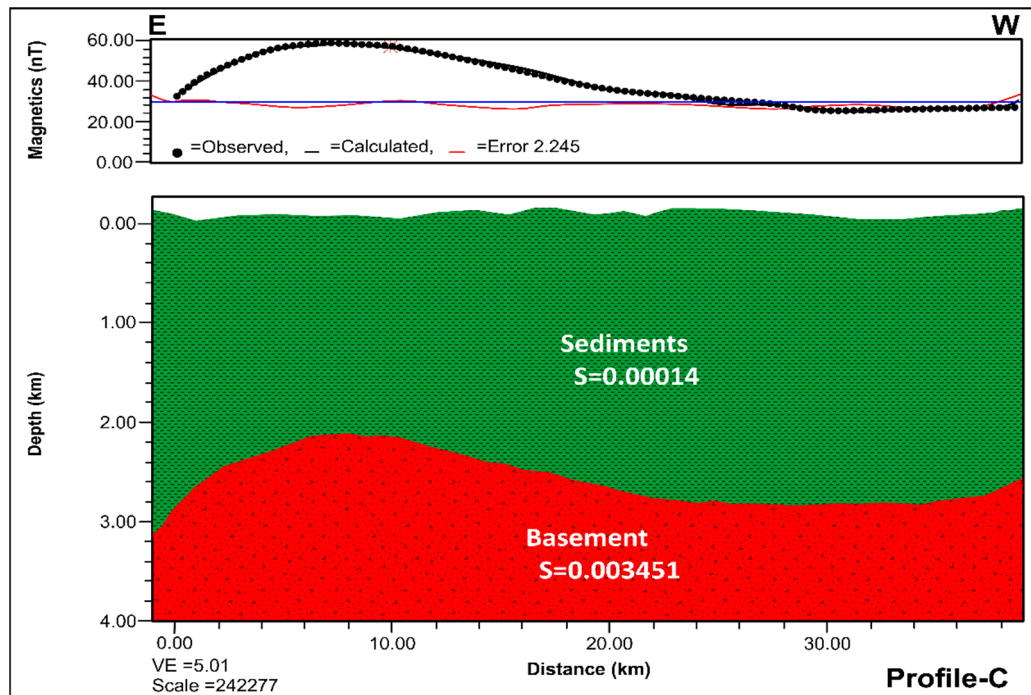


Fig. 10c 2D-Forward modelling profile C.

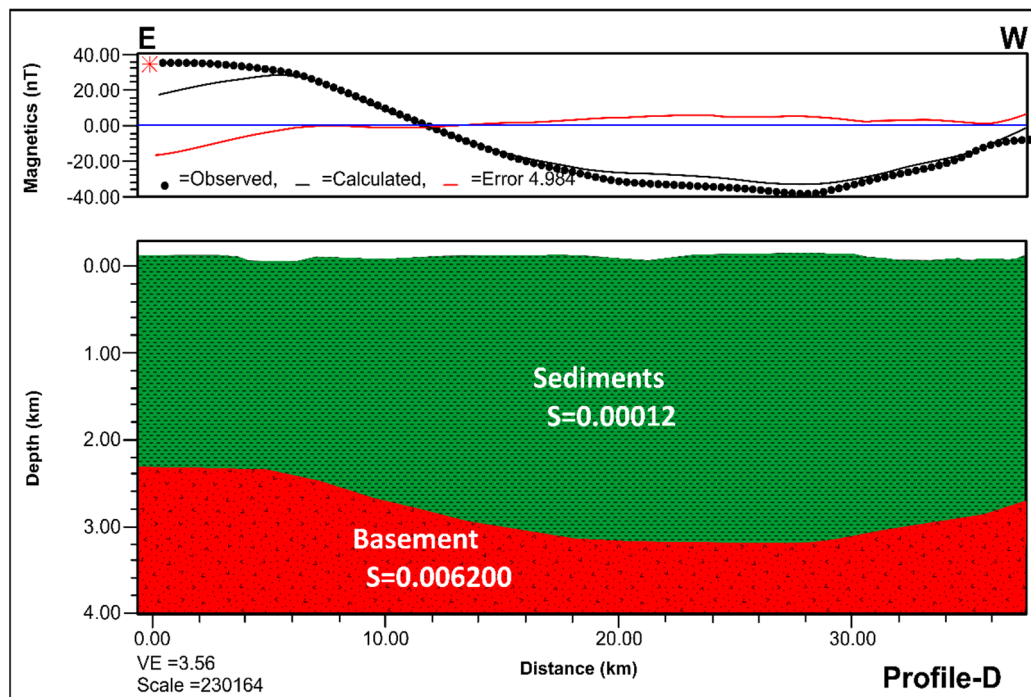


Fig. 10d 2D-Forward modelling profile D.

Baird, D.W., Aburawi, R.M. and Bailey, N.J.L.: 1996, Geohistory and petroleum in the central Sirt Basin. The geology of Sirt Basin, Proc. 1st Symposium on the Sedimentary Basins of Libya, Tripoli, 10-13 October 1993, 3, 3–56.

<https://www.tib.eu/de/suchen/id/BLCP%3ACN019519964>  
 Baaske, U.P., Tricker, P., Itterbeeck, J.V., Griffiths, H. and Pickens, J.: 2009, Gravity-induced deep-water carbonate deposits: Potential new plays in the Eocene of the Sirte Basin, Libya. Proc. 8th conference on African E&P, Petroleum Exploration Society of Great Britain/Houston Geological Society, London, 6.

Blakely, R. J.: 1996, Potential theory in gravity and magnetic applications. Cambridge University Press.

Burke, K. and Dewey, J.F.: 1973, Plume-generated triple junctions: key indicators in applying plate tectonics to old rocks. *J. Geol.*, 81, 4, 406–433.

Conant, L.C. and Goudarzi, G.H.: 1967, Stratigraphic and tectonic framework of Libya. *AAPG Bull.*, 51, 5, 719–730.

Cooper, G.R.J. and Cowan, D.R.: 2006, Enhancing potential field data using filters based on the local phase. *Comput. Geosci.*, 32, 10, 1585–1591.  
 DOI: 10.1016/j.cageo.2006.02.016

- Dogru, F., Pamukcu, O. and Özsoz, İ.: 2017, Application of tilt angle method to the Bouguer gravity data of Western Anatolia. *Bull. Miner. Res. Explor.*, 155, 213–222. DOI: 10.19111/bulletinmre.305177
- Duronio, P. and Colombi, L.: 1983, Mesozoic rocks of Libya. Spec. paper, Petroleum Exploration Society Libya.
- Eshanibli, A., Khalil, A., Younis, A. and Ghanoush, H.: 2020, Structural framework of the Zelten Platform, South Sirte Basin, Libya using potential fields modelling. *Acta Geodyn. Geomater.*, 17, 2, 229–236. DOI: 10.13168/AGG.2020.0017
- Eshanibli, A.S., Osagie, A.U., Ismail, N.A. and Ghanoush, H.B.: 2021, Analysis of gravity and aeromagnetic data to determine the structural trend and basement depth beneath the Ajdabiya Trough in northeastern Libya. *SN Appl. Sci.*, 3, 2, 1–15. DOI: 10.1007/s42452-021-04263-7
- Essed, A.S.: 1978, A reconnaissance Bouguer gravity anomaly map of Libya. Ph.D Thesis, Purdue University, United States.
- Finetti, I.: 1985, Structure and evolution of the central Mediterranean (Pelagian and Ionian Seas). In: Stanley, D.J., Wezel, F.C. (Eds.), *Geological evolution of the Mediterranean Basin*, Springer, 215–230.
- Ghanoush, H.: 2019, Structure of the Ajdabiya Trough, NE Sirt Basin, Libya, derived from gravity and magnetic data. *Int. J. Sci. Res.*, 8, 1289–1304. DOI: 10.21275/ART20195738
- Ghanoush, H., Imber, J. and McCaffrey, K.: 2014, Cenozoic subsidence and lithospheric stretching deformation of the Ajdabiya Trough Area, Northeast Sirt Basin, Libya. 2014 AAPG Annual Convention and Exhibition, Houston, Texas, USA.
- Gumati, Y.D. and Kanes, W.H.: 1985, Early Tertiary subsidence and sedimentary facies-northern Sirte Basin, Libya. *AAPG Bull.*, 69, 1, 39–52. DOI:10.1306/AD461B83-16F7-11D7-8645000102C1865D
- Hallett, D.: 2002, The Structure Geology. In: Selley, R. and Tull, S. (Eds.), *Petroleum Geology of Libya*, vol. 3, Amsterdam, Elsevier, 265–321.
- Hallett, D. and El Ghoul, A.: 1996, Oil and gas potential of the deep trough areas, in the Sirt Basin, Libya. In: Salem M.J. et al. (Eds.), *The geology of Sirt Basin*, Amsterdam, Elsevier, 454–483.
- Hallett, D. and Clark-Lowes, D.: 2017, *Petroleum geology of Libya*. Elsevier, Netherlands.
- Hinze, W.J., von Frese, R.R.B. and Saad, A.H.: 2013, Gravity and magnetic exploration principles, practices, and applications. Cambridge University Press, New York, 515 pp. DOI: 10.1017/CBO9780511843129
- Holden, E.-J., Wong, J.C., Kovesi, P., Wedge, D., Dentith, M. and Bagas, L.: 2012, Identifying structural complexity in aeromagnetic data: An image analysis approach to greenfields gold exploration. *Ore Geol. Rev.*, 46, 47–59. DOI: 10.1016/j.oregeorev.2011.11.002
- Keller, G.V.: 1986, An introduction to geophysical exploration. *Eos Trans. AGU*, 67, 11, 132–132. DOI: 10.1029/EO067i011p00132-01
- Klitzsch, E.: 1971, The structural development of parts of North Africa since Cambrian time. In: Cray, C. (Ed.), *Symposium on the Geology of Libya*, University of Libya, Tripoli, 253–262.
- Massa, D., Havlíček, V. and Bonnefous, J.: 1977, Stratigraphic and faunal data on the Ordovician of the Rhadames Basin (Libya and Tunisia). *Bull. Cent. Rech. Explor. Prod. Elf-Aquitaine*, 1, 3–27.
- Miller, H.G. and Singh, V.: 1994, Potential field tilt-a new concept for location of potential field sources. *J. Appl. Geophys.*, 32, 2-3, 213–217. DOI: 10.1016/0926-9851(94)90022-1
- Ming, Y., Ma, G., Li, L., Han, J. and Wang, T.: 2021, The spatial different order derivative method of gravity and magnetic anomalies for source distribution inversion. *Remote Sens.* 13, 5, 964. DOI: 10.3390/rs13050964
- Putri, D.R., Nanda, M., Rizal, S., Idroes, R. and Ismail, N.: 2019, Interpretation of gravity satellite data to delineate structural features connected to geothermal resources at Bur Ni Geureudong geothermal field. *IOP Conf. Series: Earth and Environmental Science*, 364, 1, 012003. DOI: 10.1088/1755-1315/364/1/012003
- Saadi, N.M., Aboud, E., Saibi, H. and Watanabe, K.: 2008, Integrating data from remote sensing, geology and gravity for geological investigation in the Tarhunah area, Northwest Libya. *Int. J. Digit. Earth*, 1, 4, 347–366. DOI: 10.1080/17538940802435844
- Saheel, A.S., Samsudin, A.R. and Hamzah, U.: 2010a, Interpretation of gravity and magnetic anomalies of the Ajdabiya Trough in the Sirte Basin, Libya. *Eur. J. Sci. Res.*, 43, 3, 316–330.
- Saheel, A.S., Samsudin, A.R. and Hamzah, U.: 2010b, Regional geological and tectonic structures of the Sirt Basin from potential field data. *Am. J. Sci. Ind. Res.*, 1, 3, 448–462. DOI: 10.5251/ajsir.2010.1.3.448.462
- Saheel, A.S., Samsudin, A.R. and Hamzah, U.: 2011, Mapping of faults in the Libyan Sirte Basin by magnetic surveys. *Sains Malays.*, 40, 8, 853–864.
- Saleem, M.A.A.: 2015, Tectonic evolution and structural analysis of south-western Sirte Basin, Central Libya. Ph.D Thesis, University of Birmingham, UK.
- Shaaban, F.F. and Ghoneimi, A.E.: 2001, Implication of seismic and borehole data for the structure, petrophysics and oil entrapment of Cretaceous-Palaeocene reservoirs, northern Sirt Basin, Libya. *J. African Earth Sci.*, 33, 1, 103–133. DOI:10.1016/S0899-5362(01)90093-4
- Talwani, M., Worzel, J.L. and Landisman, M.: 1959, Rapid gravity computations for two-dimensional bodies with application to the Mendocino submarine fracture zone. *J. Geophys. Res.*, 64, 1, 49–59. DOI:10.1029/JZ064i001p00049
- Vail, J.R.: 1991, The Precambrian tectonic structure of North Africa. In: Salem, A.M. et al. (Eds.), *The geology of Libya*, 6, 2259–2268.
- van Der Meer, F.D. and Cloetingh, S.: 1993, Intraplate stresses and the subsidence history of the Sirte Basin, Libya. *Tectonophysics*, 226, 1-4, 37–58. DOI: 10.1016/0040-1951(93)90109-W
- Wang, Y.E., Eichkiltz, Ch.G., Schreilechner, M.G., Heinemann, G., Davis, J.C. and Gharsalla, M.: 2016, Seismic attributes for description of reef growth and channel system evolution-Case study of Intisar E, Libya. *Interpretation*, 4, 1, SB1–SB11. DOI: 10.1190/INT-2015-0017.1